Optimization of microfluidic layouts as a wired packing problem

Sanjy Andriamiseza * **Mikael Trellet** * **Nicolas Lafitte** *
Charles-Henri Clerget ** **Nicolas Petit** **

* *Fluigent, 67 av. de Fontainebleau, 94270 Le Kremlin-Bicêtre, France*
** *Centre Automatique et Systèmes, MINES ParisTech, PSL University, 60 bd St Michel, 75272, France, (e-mail: nicolas.petit@mines-paristech.fr)*

Abstract This paper presents a methodology to optimize the physical layout of microfluidic components, a key step in the design of custom microfluidic instruments that can be used in various process applications. A mathematical formulation is proposed under the form of a Mixed Integer Linear Problem allowing to treat non overlapping constraints for the multi-objective optimization of layout footprint and connectivity lengths. The method is numerically tested using randomly generated scenarios. Then, a real testcase serves as illustration.

Keywords: Microfluidics, optimization, mathematical programming, device integration technologies

1. INTRODUCTION

Microfluidics is the science of manipulating and controlling fluids at Reynolds numbers lower than 1.0, in very small amounts (microliters to picoliters), in networks of channels with dimensions significantly below 1 mm (from tens to hundreds of micrometers). Microfluidic systems are used in process engineering, chemistry and biotechnology where their ability to handle small volumes with high accuracy is a key asset. Microfluidics is an enabling technology for many lab-on-chip applications such as molecular analysis, clinical diagnostic testing, virus detection and manipulation (including COVID-19, see Berkenbrock et al. (2020); Basiri et al. (2020)), DNA analysis, pathogen detection, and also in the field of synthetic chemistry and materials engineering as vast numbers of microreactors and micromixers can be created by microfluidic droplets generation (see e.g. Shallan and Priest (2019); Zhang et al. (2016); Hegab et al. (2013); Nguyen et al. (2019); Dittrich and Manz (2006); Chabert and Viovy (2008); Riche et al. (2016); Bayareh (2020); Maddala and Rengaswamy (2013); Paulson et al. (2015)).

For each considered application listed above, specific microfluidic instruments have to be designed and built. A typical microfluidic instrument is presented in Figure 1. The instruments are usually built using ideas and concepts very similar to those found in the electronic integrated circuits industry. Often, microfluidic instruments are relatively bulky and complex systems as they include a non-negligible number of macroscopic components, ranging from pumps, cells, tanks and switches, each having input and outputs ports, connected according to a flow-diagram. For the most part, the components are placed on a single
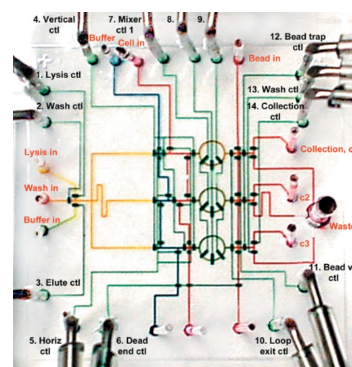

Figure 1. A microfluidic DNA purification chip Hong et al. (2004).

layer and the instruments are boxed in a rectangular enclosure.

Designing a microfluidic instrument requires to define a physical two-dimensional layout of the various components. This tasks is usually performed in a holistic way, often by referring to previously considered templates that are gradually improved through trial-and-error processes. This tedious task is very time-consuming and often results in vastly sub-optimal designs.

With the advent of the microfluidics technology and its generalized use in numerous laboratories and industries, worldwide, it has gradually become necessary to replace the trial-and-error practices by more systematic approaches. A microfluidic instrument being similar in spirit to a (micro) chemical plant, this trend is to be related to mathematical methodologies developed for optimal design, process intensification and integration that are common practices in the chemical process industry (see e.g. Swartz and Kawajiri (2019); Baldea (2015)). Following the vast literature on optimization of layout in chemical plants

---

(see e.g. Papageorgiou and Rotstein (1998) and references therein), a natural idea is to formulate the layout problem under the form of a mathematical programming problem. This is the approach we explore in this article.

Besides their geometry, which can be approximated by rectangles without too much loss of generality, an important feature of each component is its list of input and output ports (also referred to as *sockets*). A flow-diagram describes the inter-components connections. The connections between the sockets are done by microfluidic tubings. As will appear, the connectivity requires special care in the mathematical treatment.

The paper is organized as follows. In Section 2, the problem under consideration is defined, which allows to stress the similarities and differences with works from the literature. In Section 3, a mathematical formulation is presented under the form of a mixed-integer linear programming (MILP) problem. Section 4 reports numerical results and a test-case application. Finally, conclusions and perspectives are given in Section 5.

2. PROBLEM STATEMENT

2.1 Description of the WRPMP: Wired Rectangle Packing Minimization Problem

In words, the layout design consist in choosing the locations of rectangles in a plane in an optimal way, favoring the layout compactness, under the constraint that they should not overlap and that the required connections between them should be optimized. Physically, the connections between the rectangles consists of capillary tubings which are actually distributed in 3 dimensions, allowing crossing of their planar projections when necessary. To minimize holdups and hydraulic delays, their lengths matter.

Formally, the criteria to minimize define a multi-objective function consisting of the size of the rectangle encompassing the components and the length of the microfluidic connections. We will refer to this problem as "Wired Rectangle Packing Minimization Problem" (WRPMP). Figure 2 shows an optimal solution for an example problem.
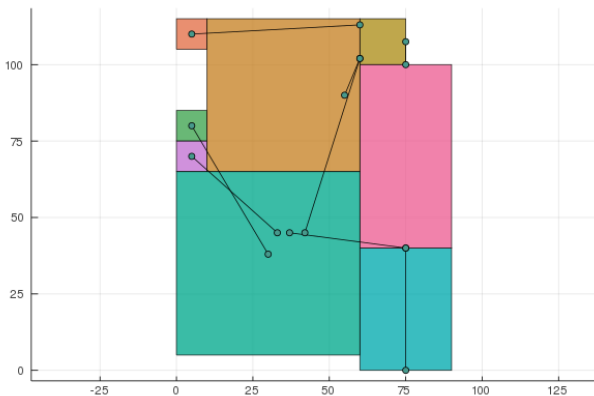

Figure 2. Solution to an example WRPMP. The reservoirs (3 top left squares) are constrained to be aligned.

2.2 Related problems from the literature

In optimization and operations research, several classic packing problems are closely related to ours. The Rectangle Packing Area Minimization Problem (RPAMP) Wu et al. (2018) treats rectangular objects of the type considered here, but ignores the connection between the components. The 2-Dimensional Bin Packing Problem (2DBPP) considers the packing without overlapping of a given set of small rectangles into the minimum number of identical large rectangles, called "bins", with the edges of the items parallel to those of the bins. It can not be employed here for the same reason as the RPAMP.

Besides, there are several domains of process engineering where similar packing problems appear, see e.g. Wu et al. (2017). The chemical process industry has a long history of solving process plant layout (PPL) problems, see e.g. Kusiak and Heragu (1987); Papageorgiou and Rotstein (1998); Westerlund et al. (2005). The PPL shares many properties and mathematical formulations with the problem at stake in this paper. While PPL problems focus on connectivity costs, and production organization through the accommodation of manufacturing patterns taking the form of bins (or production sections), the focus is not on minimizing the size of the layout, which is usually not a decision variable but a constraint. Other typical features such as safety requirements (minimum distance between some equipments) or space restrictions especially in the case of retrofit of existing plants are not found in the considered microfluidic instrument design applications.

In another area, namely microelectronics and integrated circuit, packing problems are ubiquitous. Minimization of the interconnect fabrics area is obtained by repetitive arrangement of rectangular blocks which are connected using wiring by abutment. Compared to these works, our problem has relaxed wiring constraints, as connections can be made out of the plane, allowing "jumps" and crossing of connections across the board[1]. For these reasons, our problem is more general and, therefore, has a higher mathematical complexity (for a same number of components).

3. MATHEMATICAL FORMULATION

3.1 Notations

In what follows, a microfluidic component is represented as a two-dimensional object in the xy-plane equipped with a reference axis. Its rectangular shape is defined by two strictly positive parameters L_x and L_y, and its position is defined by the coordinates (x, y) of its bottom-left point (origin of the component)[2]. Its orientation corresponds to any of the 90 degree rotation w.r.t. the reference axis.

The microfluidic component has several input and output ports, referred to as *sockets*. Each component has at least one socket. Each socket $j = 1, ..., m_i \geq 1$ of the component $i = 1, ..., N$ has a relative position defined w.r.t. the origin

---

[1] Note than in future applications, optimizing the number and the locations of crossings could be of interest, especially in the context of integration of tubings into manifolds.
[2] See e.g. Papageorgiou and Rotstein (1998) for an alternative representation
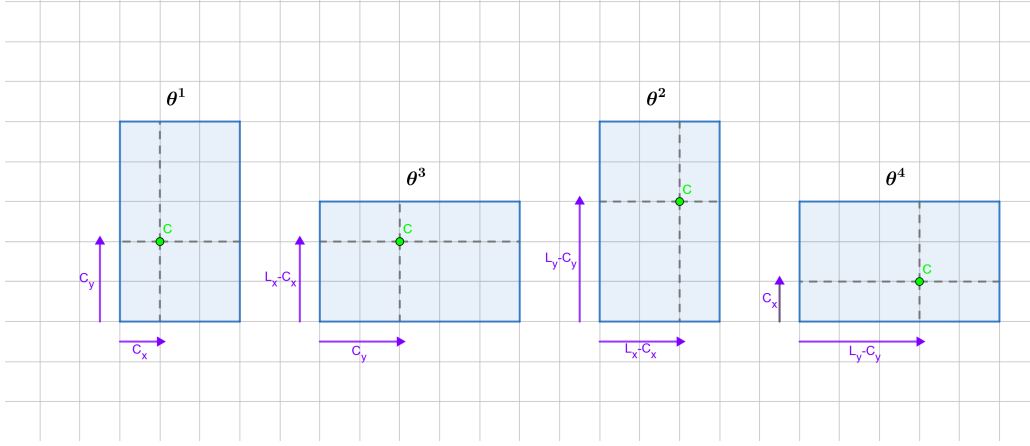
Figure 3. Representation of rectangle rotation with connectors

of the component, with two parameters Cx_{ij} and Cy_{ij}, see Figure 3. Finally, $\mathbb{B}$ is the set of Boolean variables, i.e. $\{0, 1\}$.

3.2 Non-overlapping constraints

The non-overlapping of two rectangles i and j is a disjunctive constraint. It is well-known it can be recast into a mixed-integer linear form, see e.g. Papageorgiou and Rotstein (1998). We follow this approach. To avoid overlapping, the two rectangles should have their bottom-left points sufficiently far away from each-other in the x or the y direction. Mathematically, this can be recast as follows. Consider g_{ij} and b_{ij} two Boolean variables defining the horizontal and vertical relative positions of the two rectangles:

$$g_{ij} \triangleq \begin{cases} 1 & \text{if } x_i + L_{xi} \leq x_j \\ 0 & \text{otherwise} \end{cases}$$
$$b_{ij} \triangleq \begin{cases} 1 & \text{if } y_i + L_{yi} \leq y_j \\ 0 & \text{otherwise} \end{cases}$$

Then, the non-overlapping constraint is satisfied if and only if

$$g_{ij} + g_{ji} + b_{ij} + b_{ji} \geq 1$$

Using the classic big-M method (see e.g. Papageorgiou and Rotstein (1998); Grossmann (2002)), all the non-overlapping constraints (for every $i \neq j$) can be accounted for under the form

$$x_j - x_i + M_x(1 - g_{ij}) \geq L_{xi}$$
$$y_j - y_i + M_y(1 - b_{ij}) \geq L_{yi}$$

where M_x and M_y are two large positive parameters. In the applications of this article, M_x and M_y are set to:

$(1 + \epsilon) \sum_{i=1,\dots,N}(L_{xi})$ and $(1 + \epsilon) \sum_{i=1,\dots,N}(L_{yi})$ with $\epsilon = 5e - 2$.

The big-M method could be advantageously replaced by a convex-hull method, see e.g. Grossmann and Lee (2003) to avoid overly large relaxation of actual feasible sets which can be troublesome and costly for subsequent MILP solvers.

3.3 First objective function: encompassing perimeter

It is desired to promote compactness of the layout of a set of microfluidic components. Several natural choices could

be considered to mathematically formulate this goal. All are related to the rectangle encompassing the components. The restriction to an encompassing rectangle is motivated by practical considerations, as all microfluidic instruments are eventually boxed in rectangular enclosures. For instance, the rectangle could be measured in two ways, through its area or its perimeter. The perimeter is a relevant choice as it naturally avoids extreme aspect ratios which could be generated as artifacts by minimizing the area. Mathematically, considering the perimeter is appealing as it yields a linear formulation. For example, ignoring the non-overlapping constraint for sake of clarity, the least perimeter encompassing a set of microfluidic components is defined by the following linear program:

$$\min_{z_x, z_y} \quad z_x + z_y$$
$$\text{s.t.}$$
$$z_x \geq x_i + L_{xi}, \quad i = 1, \dots, N,$$
$$z_y \geq y_i + L_{yi}, \quad i = 1, \dots, N$$

The minimum encompassing perimeter problem being translationally invariant, the coordinates of the various components must be bounded in both x and y directions. Then, with the non-overlapping constraints, the minimum encompassing perimeter problem writes

$$\min_{\substack{z_x, z_y, (x_i), (y_i), \\ (b_{ij} \in \mathbb{B}), (g_{ij} \in \mathbb{B})}} \quad z_x + z_y$$
$$\text{s.t.}$$
$$\begin{aligned}
z_x &\geq x_i + L_{xi}, & i &= 1, \dots, N, \\
z_y &\geq y_i + L_{yi}, & i &= 1, \dots, N, \quad (1) \\
x_j - x_i + M_x(1 - g_{ij}) &\geq L_{xi}, & i &\neq j, \\
y_j - y_i + M_y(1 - b_{ij}) &\geq L_{yi}, & i &\neq j, \\
g_{ij} + g_{ji} + b_{ij} + b_{ji} &\geq 1, & i &< j, \\
x_i \geq 0, y_i &\geq 0
\end{aligned}$$

3.4 Second objective function: connection lengths

The sockets of all the microfluidic components can be listed in a single array. A connectivity (adjacency) matrix defines point-to-point connectivity between the sockets. From this matrix, a cost can be defined. For each connection, the Manhattan distance between the sockets is computed, which corresponds to the tubing lengths under the assumption that the microfluidic tubings are aligned

with the axis of the xy-plane[3]. The Manhattan distance between two points A and B in the plane is $|x_A - x_B| + |y_A - y_B|$. In this expression, the absolute value function can be reformulated using an additional variables d_x and the constraints $d_x \geq (x_A - x_B)$, $d_x \geq (x_B - x_A)$. It suffices to minimize d_x to minimize $|x_A - x_B|$. This yields the generic formulation

$$\min_{d_x, d_y} \quad d_x + d_y$$
$$\text{s.t.}$$
$$d_x \geq x_A - x_B, \quad d_x \geq x_B - x_A,$$
$$d_y \geq y_A - y_B, \quad d_y \geq y_B - y_A$$

Gathering the two objectives   From the derivations above, one can now formulate an optimization problem, where, for now, the two cost objectives are simply added. This gives (2). For brevity of mathematical expressions, a $D_{iljk} \in \mathbb{B}$ is introduced. It is equal to 1 if and only if the l socket of component i is connected to the k socket of component j.

$$\min_{\substack{L,P,z_x,z_y,(x_i),(y_i),(b_{ij}\in\mathbb{B}), \\ (g_{ij}\in\mathbb{B}),(d_{xiljk}),(d_{yiljk})}} \quad L + P$$
$$\text{s.t.}$$
$$L = \sum_{i=1}^{N}\sum_{l=1}^{m_i}\sum_{j=1}^{N}\sum_{k=1}^{m_j}(d_{xiljk} + d_{yiljk})D_{iljk},$$
$$P = z_x + z_y,$$
$$z_x \geq x_i + L_{xi}, \qquad\qquad i = 1,\ldots,N,$$
$$z_y \geq y_i + L_{yi}, \qquad\qquad i = 1,\ldots,N,$$
$$x_j - x_i + M_x(1 - g_{ij}) \geq L_{xi}, \quad i \neq j,$$
$$y_j - y_i + M_y(1 - b_{ij}) \geq L_{yi}, \quad i \neq j,$$
$$g_{ij} + g_{ji} + b_{ij} + b_{ji} \geq 1, \qquad i < j,$$
$$d_{xiljk} \geq (x_i + C_{xil}) - (x_j + C_{xjk}) \quad l = 1,...,m_i,$$
$$d_{xiljk} \geq (x_j + C_{xjk}) - (x_i + C_{xil}) \quad k = 1,...,m_j,$$
$$d_{yiljk} \geq (y_i + C_{yil}) - (y_j + C_{yjk}),$$
$$d_{yiljk} \geq (y_j + C_{yjk}) - (y_i + C_{yil}),$$
$$x_i \geq 0, \, y_i \geq 0$$

$$(2)$$

3.5 Allowing rotations of the components

Generally, only 4 rotations of 90 degrees are allowed, as illustrated in Figure 3. Therefore the abscissa and ordinate of the l socket of component i can be any one of the following four

$$x_i + C_{xil}, \qquad y_i + C_{yil}$$
$$x_i + L_{xi} - C_{xil}, \qquad y_i + L_{yi} - C_{yil}$$
$$x_i + C_{yil}, \qquad y_i + L_{xil} - C_{xil}$$
$$x_i + L_{yi} - C_{yil}, \qquad y_i + C_{xil}$$

Conveniently, for each component i, four Boolean variables are introduced, such that

$$\theta_i^1 + \theta_i^2 + \theta_i^3 + \theta_i^4 = 1$$

---

[3] As an alternative, the Euclidean distance could be considered, yielding another convex problem, of quadratic nature. Tests have shown that the obtained solutions are not particularly appealing from the application point of view and do not justify the increase in computational load.

The coordinates of the l socket of component i are

$$x_i + \theta_i^1 C_{xil} + \theta_i^2(L_{xi} - C_{xil}) + \theta_i^3 C_{yil} + \theta_i^4(L_{yi} - C_{yil})$$
$$y_i + \theta_i^1 C_{yil} + \theta_i^2(L_{yi} - C_{yil}) + \theta_i^3(L_{xi} - C_{xil}) + \theta_i^4 C_{xil}$$

These new coordinates can simply replace the expressions $x_i + Cx_{il}$ and $y_i + C_{il}$ in (2) (these latter corresponding to $\theta_i^1 = 1$). It is handy to introduce another Boolean variable r_i to account for the fact than L_{xi} and L_{yi} should be exchanged only if the rotation is 90 or 270 degrees. This is simply achieved with

$$r_i = \theta_i^3 + \theta_i^4, \quad 1 - r_i = \theta_i^1 + \theta_i^2$$

As a final remark, it is important to note that the whole problem being invariant by a 90 degrees rotation, it is useful to set the orientation of one (and only one) of components. This proves critical to prevent the solver from oscillating between artificially created iso-cost solutions.

3.6 Comprehensive problem formulation

Gathering all the derivations above, the general MILP model is formulated in (3).

3.7 Pareto front

Instead of the simple addition considered to formulate (3), it is much more natural to consider the multi-objective optimization problem, and therefore to consider the Pareto front of the cost functions L and P.

To compute the Pareto front given in Figure 4, we proceed as usual, see e.g. Ehrgott (2005). First a single objective problem is solved, by considering the problem (3) formulation at the exception of the objective function which is L instead of $L + P$. This optimum has a perimeter value $\bar{P}$. Then, another problem is solved, considering again L as objective function and the additional constraint that $P \leq \bar{P} - p$, where p is a step change. Gradually, the Pareto front is thus estimated as a collection of optima.

An example of the obtained Pareto front along with two solutions along the front are pictured in Figure 4. The extreme points of the Pareto front are not satisfactory from the application viewpoint. Some trade-off has to be found. A selection along the Pareto front is made.
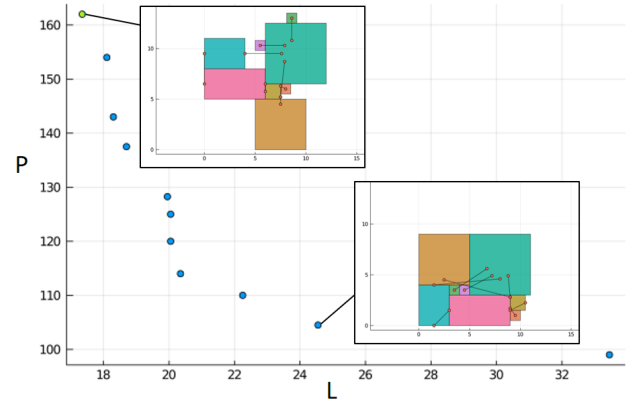

Figure 4. Pareto front and two solutions. P is the perimeter and L the total length of the wires.

$$\min_{\substack{L,P,z_x,z_y,(x_i),(y_i),(b_{ij}\in\mathbb{B}),(g_{ij}\in\mathbb{B}),\\(d_{xiljk}),(d_{yiljk}),(\theta_i^{1\cdots4}\in\mathbb{B})}} L+P$$

$$\text{s.t.}$$

$$L = \sum_{i=1}^{N}\sum_{l=1}^{m_i}\sum_{j=1}^{N}\sum_{k=1}^{m_j}(d_{xiljk}+d_{yiljk})D_{iljk},$$

$$P = z_x + z_y,$$

$$z_x \geq x_i + (\theta_i^1+\theta_i^2)L_{xi} + (\theta_i^3+\theta_i^4)L_{yi}, \qquad i=1,\dots,N,$$

$$z_y \geq y_i + (\theta_i^1+\theta_i^2)L_{yi} + (\theta_i^3+\theta_i^4)L_{xi}, \qquad i=1,\dots,N,$$

$$x_j - x_i + M_x(1-g_{ij}) \geq (\theta_i^1+\theta_i^2)L_{xi} + (\theta_i^3+\theta_i^4)L_{yi}, \qquad i\neq j,$$

$$y_j - y_i + M_y(1-b_{ij}) \geq (\theta_i^1+\theta_i^2)L_{xi} + (\theta_i^3+\theta_i^4)L_{yi}, \qquad i\neq j,$$

$$g_{ij}+g_{ji}+b_{ij}+b_{ji} \geq 1, \qquad i<j, \tag{3}$$

$$d_{xiljk} \geq x_i + \theta_i^1 C_{xil} + \theta_i^2(L_{xi}-C_{xil}) + \theta_i^3 C_{yil} + \theta_i^4(L_{yi}-C_{yil}),$$
$$\qquad - x_j + \theta_j^1 C_{xjl} + \theta_j^2(L_{xj}-C_{xjl}) + \theta_j^3 C_{yjl} + \theta_j^4(L_{yj}-C_{yjl}) \quad l=1,\dots,m_i,$$

$$d_{xiljk} \geq x_j + \theta_j^1 C_{xjl} + \theta_j^2(L_{xj}-C_{xjl}) + \theta_j^3 C_{yjl} + \theta_j^4(L_{yj}-C_{yjl}),$$
$$\qquad - x_i + \theta_i^1 C_{xil} + \theta_i^2(L_{xi}-C_{xil}) + \theta_i^3 C_{yil} + \theta_i^4(L_{yi}-C_{yil}),$$

$$d_{yiljk} \geq y_i + \theta_i^1 C_{yil} + \theta_i^2(L_{yi}-C_{yil}) + \theta_i^3(L_{xi}-C_{xil}) + \theta_i^4 C_{xil},$$
$$\qquad - y_j + \theta_j^1 C_{yjl} + \theta_j^2(L_{yj}-C_{yjl}) + \theta_j^3(L_{xj}-C_{xjl}) + \theta_j^4 C_{xjl},$$

$$d_{yiljk} \geq y_j + \theta_j^1 C_{yjl} + \theta_j^2(L_{yj}-C_{yjl}) + \theta_j^3(L_{xj}-C_{xjl}) + \theta_j^4 C_{xjl},$$
$$\qquad - y_i + \theta_i^1 C_{yil} + \theta_i^2(L_{yi}-C_{yil}) + \theta_i^3(L_{xi}-C_{xil}) + \theta_i^4 C_{xil},$$

$$x_i \geq 0,\ y_i \geq 0,$$

$$\theta_1^1 = 1, \quad \theta_i^1+\theta_i^2+\theta_i^3+\theta_i^4 = 1$$

4. RESULTS

4.1 Testing the method on random cases

Creation of relevant test cases by randomization The methodology developed in this article is implemented under the form of a software package. To assess its numerical performance (in view of generalized use), some tests must be performed to determine what is the size N that can be treated in a given time.

The performance assessment is achieved by using randomly generated cases. The randomly generated instances must have some degree of realism. Consequently, all rectangles dimensions, number and sizes of sockets correspond to real microfluidic components found off-the-shelves. Then, the connectivity graph must be randomly generated, having a prescribed degree of connection. For this, several methods can be employed, see Viger and Latapy (2005); Erdös and Rényi (1959); Molloy and Reed (1995).

A graph is a diagram of points (vertices) and lines (edges) connected to the points. The points represent the components. When two vertices are directly connected by a line, they are said to be adjacent. The degree of a vertex is the number of vertices adjacent to this vertex.

The Molloy and Reed Molloy and Reed (1995) method generates a random graph with prescribed degree sequence in linear time. However, this model produces graphs that are neither simple nor connected. A simple graph is a graph having neither multiple edges (the case of several edges binding the same pair of vertices is forbidden), nor loops, i.e. edges binding a vertex to itself. To circumvent this,

one generally simply removes multiple edges and loops, and then keeps only the largest connected component. The merits of such an approach is to handle very large networks (i.e. very large N) which is out-of-the-scope of our study.

The Watts–Strogatz (WS) model Watts and Strogatz (1998) is a random graph generation model that produces graphs with small-world properties [4], including short average path lengths (meaning that the average number of steps needed to relate two components is small) and high clustering (measure of the degree to which components in a graph tend to cluster together). This method is well-suited for our study.

To be representative of the microfluidic instruments treated in our applications, the WS model shall be used with parameters that promote short (but not too short) average path and limit clustering. The two parameters at stake are $0 \leq \beta \leq 1$ use as a probability in the WS model to create a connection and K the mean degree of the graph. Following, the results of Barrat and Weigt (2000), to reduce clustering β should be close to 1. The degree K can be set close to the maximum of connection of the components. To avoid reducing the average path too much, β should be kept relatively small.

In practice, the WS model is run with $\beta = 0.7$. If the graph is not connected, then it is discarded. Typical results obtained with the WS method are pictured in Figure 5.

Then, the sockets locations are chosen. Each vertex of the graph is a component. It has as many connected edges as it has sockets. The two dimensional parameters,

---

[4] This property is of interest for asymptotics when the number of components N is large, which is not of interest here

N	av. t	std t	min t	max t	av. a	std a	min a	max a	av. d	std d	min d	max d
3	0.14	0.024	0.08	0.20	60.58	27.5	9	121	7.69	2.9	2.09	13.79
4	0.36	0.077	0.18	0.52	91.05	31.39	30.23	165	8.13	2.85	1.86	15.44
5	0.93	0.41	0.37	2.14	138.31	49.9	39.56	246.1	10.35	4.3	3.34	24.09
6	2.39	1.64	0.57	7.47	170.85	58.5	54.34	328	10.84	3.84	4.7	19.38
7	5.11	2.16	1.59	12.6	190.76	56.48	106.82	333.6	12.03	4.12	3.71	21.4
8	10.41	7.88	1.2	42.34	258.14	79.93	66.25	436.94	14.16	5.27	3.6	27.95
9	31.44	20.96	5.09	90.61	292.64	84.14	140.16	539	15.31	5.53	4.38	32.33
10	112.16	113.56	8.52	595.66	364.17	83.77	171.6	537.94	18.71	5.33	7.2	29.67

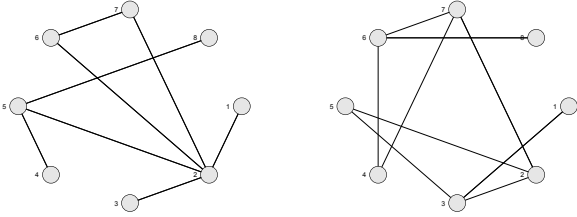Table 1. Benchmark results on 50 random instances.

Figure 5. Left: graph of the testcase treated in Figure 4. Right: a randomly generated graph.

and the locations of its sockets can be randomly chosen consistently with the database of microfluidic component found off-the-shelves discussed earlier.
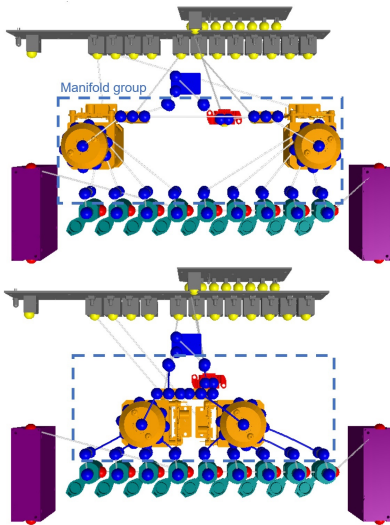

Figure 6. Optimization of the microfluidic manifold, minimizing fluidic paths (top: initial layout, bottom: optimal layout).

Numerical performance For establishing the numerical performance, all test were performed on a Intel(R) Xeon(R) E-2236 CPU @ 3.40GHz (6 cores). The following software packages were used: MILP solver is Cbc 2.10.5, see Forrest et al. (2020), which is run with Python 3.8.1 using Pyomo 5.6.8, see Hart et al. (2017). The reported computation time is the wall clock-time.

Table 1 reports the descriptive statistics obtained with 50 random instances of systems ranging from 3 to 10 connected components. Information provided are average (av.), standard deviation (std), max and min of t wall-clock time, a total area defined as $a = z_x \times z_y$ and d sum of all connection lengths.

4.2 A real test-case

We report results obtained for a real microfluidic instrument. The instrument consists of N=30 components that are 9 reservoirs connected to 2 pressure controllers, 2 electronic boards, 1 microfluidic chip, and in the middle a group of microfluidic elements containing 2 11-ports valves, 2 3-ports valves, 1 flow sensor and 11 connectors (Figure 7). This latter group allows to inject, recirculate, flush fluids into the chip and is to be integrated into a microfluidic manifold.

First, the optimization method is run on the manifold assigning the 11 connectors to given positions chosen by the designer. The optimal solution minimizing microfluidic paths, and so internal volumes, is explored (Figure 6). After integration with the manifold card, all the components are optimized considering this time the manifold group and the reservoirs locations as given (i.e. 25 components) (Figure 8). The software pipeline is automated so that the designer can manipulate any of the 25 elements (if needed) and run optimization in few minutes.

For the first run with N=5 (and 11 fixed components), a Pareto front is computed using a total of 10 runs. The total computation time is about 3 seconds. An optimal trade-off is manually selected by considering number of crossings (the obtained number is zero in this case), covering, aspect ratio and sum of connection lengths. The second run N=5 (and 25 fixed components) is run in less than 3 seconds. This yields the optimal layout presented in Figure 8.

5. CONCLUSION

The main contribution of the article is a methodology to optimize the layout of microfluidic instruments by considering the two objective of minimum encompassing perimeter and total connection lengths. Following results from the literature, the mathematical formulation results in a MILP. It is shown that for typical applications of microfluidic instrument design, implementation with commonly available software packages yields satisfactory numerical results, allowing to compute the Pareto front with a good level of accuracy and a limited computation time. Having the possibility to estimate the Pareto front is a valuable asset for design engineers which can then easily determine a practical solution to the multi-objective problem. We have mentioned that our current problem does not have to account for the locations and numbers

Figure 7. Real test-case schematic circuit. Two regions are defined: the *fluidic manifold* part and the external layout part.

Figure 8. Final optimized layout of the microfluidic instrument schematized in Figure 7.

of tube crossings a system can present. However, in future applications, optimizing the number and the locations of crossings could be of interest, especially in the context of integration of tubing into manifolds. This integration could be done by adding some intersection constraints, disabling any crossing of two connections based on their connector positions.

For very large systems (more that 20 components) the methods scale poorly. However, it is often possible to decompose the system into sub-blocks of smaller sizes. The methodology allows to start with subsystems and then consider their optimized versions as new components for the next stage of the optimization procedure. This multi-stage procedure has been illustrated on a real-test case. If subsystems can not be identified, it is possible to restrict the computational time. Besides the simple strategy consisting of returning the solution after a time-out, it is possible to develop alternative methods, such as heuristics (see e.g. Bottlik (2017)), e.g. random pairwise exchange, simulated annealing (under the form of relaxing spaces between components of locally optimal solutions),

Monte-Carlo methods for initialization, or meta-heuristics, e.g. based on successive inclusion of components in the problem.

To assess the relevance of such sub-optimal strategies, intense testing on random cases can be used. The description of the random cases generator is a second contribution of the article.

REFERENCES

Baldea, M. (2015). From process integration to process intensification. *Computers & Chemical Engineering*, 81, 104–114.

Barrat, A. and Weigt, M. (2000). On the properties of small-world network models. *The European Physical Journal B-Condensed Matter and Complex Systems*, 13(3), 547–560.

Basiri, A., Heidari, A., Nadi, M.F., Fallahy, M.T.P., Nezamabadi, S.S., Sedighi, M., Saghazadeh, A., and Rezaei, N. (2020). Microfluidic devices for detection of RNA viruses. *Reviews in medical virology*, e2154.

Bayareh, M. (2020). An updated review on particle separation in passive microfluidic devices. *Chemical Engineering and Processing - Process Intensification*, 153, 107984.

Berkenbrock, J.A., Grecco-Machado, R., and Achenbach, S. (2020). Arsenal of microfluidic testing devices may combat COVID-19 pandemic. *MRS Bulletin, Cambridge University Press*, 45(7), 511–514.

Bottlik, G. (2017). *An Introduction to the Mathematics of Planning and Scheduling*. Taylor & Francis.

Chabert, M. and Viovy, J.L. (2008). Microfluidic high-throughput encapsulation and hydrodynamic self-sorting of single cells. *Proceedings of the National Academy of Sciences*, 105(9), 3191–3196.

Dittrich, P.S. and Manz, A. (2006). Lab-on-a-chip: microfluidics in drug discovery. *Nature reviews Drug discovery*, 5(3), 210–218.

Ehrgott, M. (2005). *Multicriteria optimization*, volume 491. Springer Science & Business Media.

Erdös, P. and Rényi, A. (1959). On random graphs I. *Publ. Math. Debrecen*, 6.

Forrest, J.J., Vigerske, S., Santos, H.G., Ralphs, T., Hafer, L., Kristjansson, B., Fasano, J.P., Straver, E., Lubin, M., Lougee, R., Goncal, J.P., Gassmann, H.I., and Saltzman, M. (2020). coin-or/cbc: Version 2.10.5. URL https://doi.org/10.5281/zenodo.3700700.

Grossmann, I.E. (2002). Review of nonlinear mixed-integer and disjunctive programming techniques. *Optimization and engineering*, 3(3), 227–252.

Grossmann, I.E. and Lee, S. (2003). Generalized convex disjunctive programming: Nonlinear convex hull relaxation. *Computational optimization and applications*, 26(1), 83–100.

Hart, W.E., Laird, C.D., Watson, J.P., Woodruff, D.L., Hackebeil, G.A., Nicholson, B.L., and Siirola, J.D. (2017). *Pyomo–optimization modeling in python*, volume 67. Springer Science & Business Media, second edition.

Hegab, H.M., ElMekawy, A., and Stakenborg, T. (2013). Review of microfluidic microbioreactor technology for high-throughput submerged microbiological cultivation. *Biomicrofluidics*, 7(2), 021502.

Hong, J.W., Studer, V., Hang, G., Anderson, W.F., and Quake, S.R. (2004). A nanoliter-scale nucleic acid processor with parallel architecture. *Nature biotechnology*, 22(4), 435–439.

Kusiak, A. and Heragu, S.S. (1987). The facility layout problem. *European Journal of operational research*, 29(3), 229–251.

Maddala, J. and Rengaswamy, R. (2013). Droplet digital signal generation in microfluidic networks using model predictive control. *Journal of Process Control*, 23(2), 132 – 139. IFAC World Congress Special Issue.

Molloy, M. and Reed, B. (1995). A critical point for random graphs with a given degree sequence. *Random structures & algorithms*, 6(2-3), 161–180.

Nguyen, N.T., Wereley, S.T., and Shaegh, S.A.M. (2019). *Fundamentals and applications of microfluidics*. Artech house.

Papageorgiou, L.G. and Rotstein, G.E. (1998). Continuous-domain mathematical models for optimal process plant layout. *Industrial & engineering chemistry research*, 37(9), 3631–3639.

Paulson, J.A., Mesbah, A., Zhu, X., Molaro, M.C., and Braatz, R.D. (2015). Control of self-assembly in micro- and nano-scale systems. *Journal of Process Control*, 27, 38 – 49.

Riche, C.T., Roberts, E.J., Gupta, M., Brutchey, R.L., and Malmstadt, N. (2016). Flow invariant droplet formation for stable parallel microreactors. *Nature communications*, 7(1), 1–7.

Shallan, A.I. and Priest, C. (2019). Microfluidic process intensification for synthesis and formulation in the pharmaceutical industry. *Chemical Engineering and Processing - Process Intensification*, 142, 107559.

Swartz, C.L. and Kawajiri, Y. (2019). Design for dynamic operation-a review and new perspectives for an increasingly dynamic plant operating environment. *Computers & Chemical Engineering*, 128, 329–339.

Viger, F. and Latapy, M. (2005). Efficient and simple generation of random simple connected graphs with prescribed degree sequence. In *International Computing and Combinatorics Conference*, 440–449. Springer.

Watts, D.J. and Strogatz, S.H. (1998). Collective dynamics of small-world networks. *nature*, 393(6684), 440–442.

Westerlund, J., Papageorgiou, L.G., and Westerlund, T. (2005). A problem formulation for optimal mixed-sized box packing. In *Computer Aided Chemical Engineering*, volume 20, 913–918. Elsevier.

Wu, L., Liu, Q., Wang, F., Xiao, W., and Yang, Y. (2018). Heuristic algorithm for RPAMP with central rectangle and its application to solve oil-gas treatment facility layout problem. *Eng. Appl. Artif. Intell.*, 72, 294–309.

Wu, L., Tian, X., Zhang, J., Liu, Q., Xiao, W., and Yang, Y. (2017). An improved heuristic algorithm for 2d rectangle packing area minimization problems with central rectangles. *Engineering Applications of Artificial Intelligence*, 66, 1–16.

Zhang, J., Yan, S., Yuan, D., Alici, G., Nguyen, N.T., Warkiani, M.E., and Li, W. (2016). Fundamentals and applications of inertial microfluidics: a review. *Lab on a Chip*, 16(1), 10–34.